Journal of Organometallic Chemistry, 452 (1993) 205–218

JOM 23320

Coordination chemistry of $[CH_2(PPh_2)(P(Y)R_2)]$ and $[CH(PPh_2)(P(Y)R_2)]^-$, Y = S or Se, R = Ph or ^{t}Bu: rhodium, iridium and ruthenium complexes; ^{13}C, ^{31}P, and ^{77}Se NMR studies; and the crystal and molecular structures of $[Ir(cod)\{CH_2(PPh_2)(P(S)^tBu_2)\text{-}P,S\}]BF_4 \cdot CHCl_3$, $[Rh(cod)\{CH_2(PPh_2)(P(S)^tBu_2)\text{-}P,S\}]ClO_4 \cdot CH_2Cl_2$, $[Rh(cod)\{CH(PPh_2)(P(S)Ph_2)\text{-}P,S\}]$, and $[RuCl_2(p\text{-cymene})\{CH_2(PPh_2)(P(S)Ph_2)\text{-}P\}] \cdot CH_2Cl_2$

Jane Browning, Gordon W. Bushnell, Keith R. Dixon and Robert W. Hilts

Department of Chemistry, University of Victoria, Victoria, B.C., V8W 3P6 (Canada)

(Received July 7, 1992; in revised form October 19, 1992)

Abstract

Reactions of the chloro-bridged complexes, $[M_2Cl_2(cod)_2]$, M = Ir or Rh, COD = cyclooctadiene, with $CH_2(PPh_2)(P(Y)R_2)$, Y = S or Se, R = Ph or ^{t}Bu, provide a synthetic route to the cations, $[M(cod)\{CH_2(PPh_2)(P(Y)R_2)\text{-}P,S\}]^+$, which are isolated as fluoroborate or perchlorate salts. Treatment of these products with sodium hydride results in facile deprotonation to the neutral complexes, $[M(cod)\{CH(PPh_2)(P(Y)Ph_2)\text{-}P,S\}]$, and when Y = S, the neutral complexes are also accessible via reactions of $[M_2Cl_2(cod)_2]$ with $Li[CH(PPh_2)(P(S)R_2)]$. Reactions of the cations, $[M(cod)\{CH_2(PPh_2)(P(S)^tBu_2)\text{-}P,S\}]^+$ with other ligands, Lg = $(CO)_2$, $(CN^tBu)_2$, or bis(diphenylphosphino)methane (dppm), result in displacement of cod to form $[M(Lg)\{CH_2(PPh_2)(P(S)^tBu_2)\text{-}P,S\}]^+$. Ruthenium complexes of $CH_2(PPh_2)(P(S)Ph_2)$ are accessible *via* similar bridge cleavage reactions using $[Ru_2Cl_4L_2]$, L = benzene or *p*-cymene. These complexes are characterized by complete ^{13}C, ^{31}P, and ^{77}Se nuclear magnetic resonance (NMR) studies and by four crystal structure determinations. The complexes $[Ir(cod)\{CH_2(PPh_2)(P(S)^tBu_2)\text{-}P,S\}]BF_4 \cdot CHCl_3$ (1), $[Rh(cod)\{CH_2(PPh_2)(P(S)^tBu_2)\text{-}P,S\}]ClO_4 \cdot CH_2Cl_2$ (2), $[Rh(cod)\{CH(PPh_2)(P(S)Ph_2)\text{-}P,S\}]$ (3) and $[RuCl_2(p\text{-cymene})\{CH_2(PPh_2)(P(S)Ph_2)\text{-}P\}] \cdot CH_2Cl_2$ (4) crystallize in the $P\bar{1}$ (No. 2) space group ($Z = 2$) with respective unit cells: $a = 12.307(7)$ Å, $b = 14.743(8)$ Å, $c = 10.877(6)$ Å, $\alpha = 74.42(5)°$, $\beta = 107.65(6)°$, $\gamma = 105.47(5)°$; $a = 12.163(1)$ Å, $b = 14.56(1)$ Å, $c = 10.560(1)$ Å, $\alpha = 77.69(1)°$, $\beta = 74.54(1)°$, $\gamma = 77.01(1)°$; $a = 10.650(4)$ Å, $b = 13.327(4)$ Å, $c = 10.419(3)$ Å, $\alpha = 90.60(3)°$, $\beta = 102.64(3)°$, $\gamma = 83.15(3)°$; $a = 11.217(2)$ Å, $b = 17.124(3)$ Å, $c = 10.412(2)$ Å, $\alpha = 90.58(1)°$, $\beta = 112.29(2)°$, $\gamma = 97.53(2)°$. Complexes 1–3 all contain bidentate *P,S*-bonded ligands occupying two coordination positions of an approximately square planar metal centre. In each case, the coordination is completed by two double bonds of a cod ligand. In contrast, complex 4 contains a monodentate *P*-bonded ligand.

1. Introduction

Coordination chemistry of the potentially bidentate ligands, $[CH_2(PR_2)(P(Y)R_2)]$, Y = S or Se, was first developed by Grim and co-workers about 1980 [1–4]. These early reports focused on synthetic and nuclear magnetic resonance (NMR) studies of chromium, molybdenum, and tungsten complexes. Subsequently, these same metals have been studied by other authors [5,6]. More recent work also includes complexes of mercury [7,8], palladium [9,10], platinum [9,11,12], and gold [13], with X-ray diffraction studies of $[PtCl(PEt_3)\{CH_2(PPh_2)(P(S)^tBu_2)\text{-}P,S\}]ClO_4$ [9] and $[Pd(CN)(SeCN)\{CH_2(PPh_2)(P(Se)Ph_2)\text{-}P,S\}]$ [10]. Several of these studies [9,11,13] also include complexes of the anionic ligands, $[CH(PR_2)(P(Y)R_2)]^-$, derived by deprotonation at the methylene carbon, and one of these,

Correspondence to: Professor K.R. Dixon.

0022-328X/93/$6.00

$[Au(C_6F_5)_2\{CH(PPh_2)(P(S)Ph_2)\text{-}P,S\}]$, has been studied by X-ray diffraction [13].

Most recently, interest in phosphorus chalcogenides has been maintained and accelerated by reports that ligands of these types may be effective in promoting catalysis at metal centres. For example: the *P,O* chelate complex, $[RhCl(CO)\{Ph_2PCH_2CH_2P(O)Ph_2\}]$, catalyzes carbonylation of methanol [14]; and iridium complexes of $[C(P(O)Ph_2)_3]^-$ are active in alkyne hydrosilylation [15]. Mechanisms for these catalytic processes may involve the temporary cleavage of the relatively labile metal–chalcogen bonds [14], a process which is conveniently studied in systems where the phosphorus chalcogenide ligand is also anchored to the metal by another relatively strong bond [16–18]. The present ligands, $[CH_2(PPh_2)(P(Y)R_2)]$, are examples of this possibility since the most likely mode of coordination is a five-membered chelate ring with a strong bond to the PR_2 group and a weaker bond to the Y atom.

Complexes of the ligands, $[CH_n(PR_2)(P(Y)R_2)]^{(2-n)-}$, with the catalytically important metals, rhodium, iridium and ruthenium, had not been studied prior to our work. In a preliminary communication we have noted sequential two centre reactivity of methyl iodide with $[Rh(cod)\{CH(PPh_2)(P(S)Ph_2)\text{-}P,S\}]$, where one site is the methine carbon of the ligand and the other is the metal centre [19]. The present paper describes our basic synthetic procedures, NMR studies, and four X-ray diffraction studies (Scheme 1: structures **1–4**) which serve to characterize three different coordination modes: *P,S*-chelation of neutral ligand; *P,S*-chelation of monoanion; and monodentate, *P*-coordination of neutral ligand.

2. Experimental section

2.1. Synthesis and spectroscopic studies

Data relating to the characterization of the complexes are given in the Tables, the Results section and in the preparative descriptions below. Microanalysis was by the Canadian Microanalytical Service, Vancouver, B.C., Canada. ^{31}P NMR spectra were recorded in

TABLE 1. Phosphorus-31 nuclear magnetic resonance parameters for the ligands, $[CH_n(P_APh_2)(P_B(Y)R_2)]^{(2-n)-}$, and the Complexes, $[M(Lg)\{CH_n(P_APh_2)(P_B(Y)R_2)\}]^{m+}$

M	Lg	Y	R	*n*	*m*	Notes	$\delta(P_A)$	$\delta(P_B)$	$J(P_A\text{–}P_B)$	$J(Rh\text{–}P_A)$
		S	Ph	2		[a]	−27.9	40.4	76	
		S	Ph	1		[b]	−10.2	51.0	163	
		Se	Ph	2		[a]	−27.0	30.8	83	
		S	^{t}Bu	2		[a]	−24.6	75.9	53	
		S	^{t}Bu	1		[b]	−5.7	89.4	132	
Rh	cod	S	Ph	2	1	[ac]	40.2	57.9	51	148
Rh	cod	S	Ph	1	0	[d]	41.6	54.2	121	137
Ir	cod	S	Ph	2	1	[ac]	30.1	62.3	45	
Ir	cod	S	Ph	1	0	[d]	36.7	59.4	112	
Rh	cod	S	^{t}Bu	2	1	[ae]	46.5	100.8	30	150
Rh	cod	S	^{t}Bu	1	0	[d]	46.4	95.0	88	139
Ir	cod	S	^{t}Bu	2	1	[ac]	40.9	107.2	26	
Ir	cod	S	^{t}Bu	1	0	[d]	41.7	99.4	81	
Rh	$(CO)_2$	S	^{t}Bu	2	1	[acf]	49.9	111.2	27	120
Ir	$(CO)_2$	S	^{t}Bu	2	1	[ac]	43.6	116.1	23	
Rh	$(CN^tBu)_2$	S	^{t}Bu	2	1	[acg]	54.5	110.5	43	131
Rh	dppm	S	^{t}Bu	2	1	[chi]	52.1	107.8	50	135
Rh	cod	Se	Ph	2	1	[aej]	43.2	39.1	57	148
Rh	cod	Se	Ph	1	0	[dk]	45.2	30.2	129	136
Ir	cod	Se	Ph	2	1	[acl]	33.9	41.8	51	
Rh	cod	S	Ph	1	0	[bm]	45.4	50.5	39	172
Ru	$bzCl_2$	S	Ph	2	0	[an]	23.6	34.7	37	
Ru	bzCl	S	Ph	2	1	[chn]	51.6	58.1	35	
Ru	$cmCl_2$	S	Ph	2	0	[ao]	22.6	34.7	37	
Ru	cmCl	S	Ph	1	0	[bo]	46.2	56.4	107	

The atom labels are shown in Scheme 2. Chemical shifts (δ) are quoted in parts per million relative to 85% H_3PO_4. Coupling constants (J) are in Hz.

[a] $CDCl_3$ solution; [b] tetrahydrofuran solution with external C_6D_6 lock; [c] BF_4^- salt; [d] C_6D_6 solution; [e] ClO_4^- salt; [f] $^2J(Rh\text{–}P_B)$ 2 Hz; [g] $^2J(Rh\text{–}P_B)$ 3 Hz; [h] CD_2Cl_2 solution; [i] dppm = $Ph_2P_CCH_2P_DPh_2$ where P_C is *trans* to S and P_D is *trans* to P_A. $\delta(P_C)$ −18.0 ppm, $\delta(P_D)$ −29.1 ppm, $J(P_A\text{–}P_C)$ 26 Hz, $J(P_A\text{–}P_D)$ 354 Hz, $J(P_B\text{–}P_C)$ 5 Hz, $J(P_B\text{–}P_D)$ 39 Hz, $J(P_C\text{–}P_D)$ 96 Hz, $J(Rh\text{–}P_B)$ 5 Hz, $J(Rh\text{–}P_C)$ 145 Hz, $J(Rh\text{–}P_D)$ 115 Hz; [j] $J(Se\text{–}P_B)$ 549 Hz; [k] $J(Se\text{–}P_B)$ 442 Hz; [l] $J(Se\text{–}P_B)$ 530 Hz; [m] $[Rh(cod)\{CH(SnMe_3)(PPh_2)(P(S)Ph_2)\}]Cl$, $J(Sn\text{–}P_A)$ 72.0 Hz, $J(Sn\text{–}P_B)$ 72.4 Hz, no resolution observed between ^{117}Sn and ^{119}Sn couplings; [n] bz = benzene; [o] cm = *p*-cymene.

TABLE 2. Carbon-13 nuclear magnetic resonance parameters for the ligands, $[CH_n(P_APh_2)(P_B(Y)R_2)]^{(2-n)-}$, and the complexes, $[M(cod)\{CH_n(P_APh_2)(P_B(Y)R_2)\}]^{(n-1)+}$

M	Y	R	n	Notes [a]	$\delta(C_A)$	$\delta(C_B)$	$\delta(C_C)$	$\delta(C_D)$	$\delta(C_E)$	$J(P_A-C_A)$	$J(P_B-C_A)$	$J(P_A-C_B)$	$J(Rh-C_B)$	$J(Rh-C_C)$
	S	Ph	2	b	34.9					32	55			
	S	Ph	1	c	19.7					18	116			
	S	^{t}Bu	2	b	24.6					31	39			
	Se	Ph	2	b	35.2					32	47			
Rh	S	Ph	2	bd	38.5	103.9	79.0	28.9	32.4	18	55	8	8	12
Rh	S	Ph	1	f	26.3	96.9	69.4	29.2	32.7	59	119	5	5	10
Ir	S	Ph	2	bd	37.7	92.6	63.2	29.5	32.9	25	56	13		
Ir	S	Ph	1	f	26.1	83.3	60.2	29.9	33.2	68	122	14		
Rh	S	^{t}Bu	2	beq	28.4	103.3	79.6	28.2	32.4	22	41	11	7	12
Rh	S	^{t}Bu	1	fh	16.4	96.5	75.2	29.4	32.9	63	103	12	7	12
Ir	S	^{t}Bu	2	bei	28.2	92.3	63.8	29.7	32.8	25	40	13		
Ir	S	^{t}Bu	1	fj	16.6	82.7	59.3	30.1	33.4	73	104	14		
Rh	Se	Ph	2	be	39.3	102.0	79.2	29.1	32.3	20	50	8	8	12
Rh	Se	Ph	1	f	27.9	94.8	76.4	29.4	32.6	58	110	5	5	12
Ir	Se	Ph	2	bd	38.6	90.3	63.0	29.7	32.7	25	50	13		

The atom labels are shown in Scheme 2. Chemical shifts (δ) are quoted in parts per million relative to $Si(CH_3)_3$. Coupling constants (J) are in Hz.

[a] In addition to the listed resonances, all complexes showed absortion in the phenyl carbon region, 124–134 ppm; [b] $CDCl_3$ solution; [c] Li^+ salt, d_8-tetrahydrofuran solution; [d] BF_4^- salt; [e] ClO_4^- salt; [f] C_6D_6 solution; [g] $\delta(CMe_3)$ 38.3 ppm, $\delta(CCH_3)$ 27.5 ppm, $^1J(P-CMe_3)$ 34 Hz; [h] $\delta(CMe_3)$ 38.6 ppm, $\delta(CCH_3)$ 28.7 ppm, $^1J(P-CMe_3)$ not resolved; [i] $\delta(CMe_3)$ 38.1 ppm, $\delta(CCH_3)$ 27.5 ppm, $^1J(P-CMe_3)$ 32 Hz; [j] $\delta(CMe_3)$ 38.5 ppm, $\delta(CCH_3)$ 28.7 ppm, $^1J(P-CMe_3)$ 43 Hz.

appropriate solvents (Tables 1, 2) at either 24.3 MHz using a Nicolet TT14 Fourier transform spectrometer with a Varian HA60 magnet and an external C_6D_6 lock signal or at 101.3 MHz using a Bruker WP250 Fourier transform spectrometer locked to the solvent deuterium resonance. ^{13}C and ^{77}Se spectra were recorded at 62.9 and 47.7 MHz respectively, in $CDCl_3$ solution using the Bruker instrument. For all nuclei protons were decoupled by broad band ("noise") irradiation at appropriate frequencies. ^{31}P chemical shifts were measured relative to external $P(OMe)_3$ and are reported in parts per million relative to 85% H_3PO_4 using a conversion factor of +141 ppm. ^{13}C and ^{77}Se chemical shifts are reported in ppm relative to $Si(CH_3)_4$ and $Se(CH_3)_2$ (19.071523 MHz [20]) * respectively. Positive values are deshielded relative to the references. Simulated NMR spectra were calculated using a locally constructed program package based on the UEAITR and NMRPLOT programs from the literature [21,22].

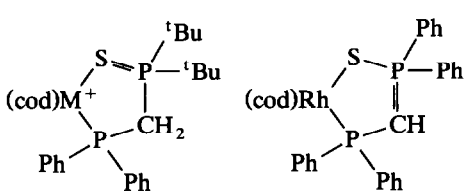

1 M = Ir
2 M = Rh

3

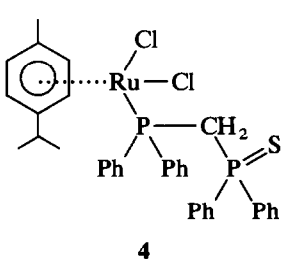

4

Scheme 1. Structures 1–4.

All operations were carried out at ambient temperature (*ca.* 25°C) under an atmosphere of dry nitrogen using standard Schlenk tube techniques. Solvents were dried by reflux over appropriate reagents (calcium hydride for dichloromethane, molecular sieves or K_2CO_3 for acetone, and potassium/benzophenone for diethyl ether, tetrahydrofuran, toluene, benzene and hexane) and were distilled under nitrogen prior to use. Recrystallizations from solvent pairs were by dissolution of the complex in the first solvent (using about double the volume required for complete solution) followed by dropwise addition of sufficient second solvent to cause turbidity at ambient temperature. Crystallization was then completed either by continued very slow dropwise addition of the second solvent or by setting the mixture aside at a reduced temperature.

The metal complexes, $[M_2Cl_2(cod)_2]$, M = Rh or Ir, and $[Ru_2Cl_4L_2]$, L = benzene or *p*-cymene, were pre-

* This value is misquoted as 19.091523 MHz in the widely used secondary reference, C. McFarlane and W. McFarlane. in R.K. Harris and B.E. Mann (eds.), *NMR and the Periodic Table*, Academic Press, London, 1978, p. 402.

pared as previously described [23–26], as were the ligands $[CH_2(PPh_2)(P(Y)R_2)]$, Y = S or Se, R = Ph or ^{t}Bu [1,2,9]. The lithium salts $Li[CH(PPh_2)(P(S)R_2)]$, R = Ph or ^{t}Bu, were prepared as previously described [9] by dropwise addition of a slight excess (*ca.* 1.1–1.2 molar equivalents) of n-butyl lithium (1.5 M in hexane) to stirred solutions of $[CH_2(PPh_2)(P(S)R_2)]$ in tetrahydrofuran. ^{31}P and ^{13}C NMR spectra confirmed that the required anions were the sole phosphorus containing products and the solutions were used without further treatment.

2.1.1. $[Rh(cod)\{CH_2(PPh_2)(P(S)^tBu_2)$-P,S$\}]ClO_4$

A solution of $CH_2(PPh_2)(P(S)^tBu_2)$ (0.20 g, 0.53 mmol) in acetone (10 ml) was added dropwise to a stirred solution of $[Rh_2Cl_2(cod)_2]$ (0.13 g, 0.26 mmol) and $NaClO_4 \cdot H_2O$ (0.078 g, 0.56 mmol) in acetone (25 ml). After 2 h the solution was filtered to remove precipitated NaCl. Solvent was removed from the filtrate *in vacuo* and the residue washed with diethyl ether (2 × 10 ml) and recrystallized from dichloromethane/diethyl ether to give $[Rh(cod)\{CH_2(PPh_2)$-$(P(S)^tBu_2)$-*P,S*$\}]ClO_4 \cdot CH_2Cl_2$ as yellow crystals (0.19 g, 0.25 mmol). Anal. Found: C, 46.5; H, 5.70. Calcd. for $C_{30}H_{44}Cl_3O_4P_2RhS$: C, 46.7; H, 5.75%.

The following complexes of the general type $[M(cod)\{CH_2(PPh_2)(P(Y)R_2)$-*P,S*$\}]$, were prepared by procedures similar to that used for the example above except that recrystallizations were from dichloromethane/hexane:

$[Ir(cod)\{CH_2(PPh_2)(P(S)^tBu_2)$-*P,S*$\}]BF_4$. Yield: 78% as dichloromethane solvate. Anal. Calcd. for $C_{30}H_{44}$-$BCl_2F_4P_2IrS$: C, 42.5; H, 5.23. Found: C, 42.3; H, 5.23%.

$[Rh(cod)\{CH_2(PPh_2)(P(S)Ph_2)$-*P,S*$\}]BF_4$. Yield: 58%. Anal. Calcd. for $C_{33}H_{34}BF_4P_2RhS$: C, 55.5; H, 4.80. Found: C, 56.2; H, 4.22%.

$[Ir(cod)\{CH_2(PPh_2)(P(S)Ph_2)$-*P,S*$\}]BF_4$. Yield: 77%. Anal. Calcd. for $C_{33}H_{34}BF_4P_2IrS$: C, 49.3; H, 4.26. Found: C, 48.7; H, 4.26%.

$[Rh(cod)\{CH_2(PPh_2)(P(Se)Ph_2)$-*P,Se*$\}]BF_4$. Yield: 58% as dichloromethane solvate. Anal. Calcd. for $C_{34}H_{36}BCl_2F_4P_2RhSe$: C, 48.3; H, 4.29. Found: C, 49.0; H, 4.38%. ^{77}Se NMR ($CDCl_3$): This spectrum consists basically of a doublet of doublets due to ^1J(Se–P_B) and ^1J(Rh–Se). However, strong coupling between the phosphorus atoms produces extra lines and distortions due to a non-first order ABMX spin system (A,B = P, M = Rh, X = Se) and a computer simulation was carried out to confirm the assignment. δ(Se) 70.2 ppm, ^1J(Se–P_B) 553 Hz, ^3J(Se–P_A) −2 Hz, ^1J(Rh–Se) 23 Hz.

$[Ir(cod)\{CH_2(PPh_2)(P(Se)Ph_2)$-*P,Se*$\}]BF_4$. Yield: 68% as dichloromethane solvate. Anal. Calcd. for $C_{34}H_{36}BCl_2F_4P_2IrSe$: C, 43.7; H, 3.88. Found: C, 44.1; H, 3.94%. This compound was also inadvertently prepared by the reaction of $CH_2\{P(Se)Ph_2\}_2$ with $[Ir_2Cl_2$-$(cod)_2]$ in the presence of $NaBF_4$ in acetone. ^{77}Se NMR ($CDCl_3$): δ(Se) 133.2 ppm, ^1J(Se–P_B) 533 Hz.

2.1.2. $[Rh(cod)\{CH(PPh_2)(P(S)Ph_2)$-P,S$\}]$

Method A: Sodium hydride (0.08 g, 2.7 mmol, 80% in oil) was added to a stirred solution of $[Rh(cod)\{CH_2$-$(PPh_2)(P(S)Ph_2)$-*P,S*$\}]BF_4$ (0.25 g, 0.35 mmol) in tetrahydrofuran (10 ml). After 2 h the reaction mixture was filtered to remove unreacted NaH. Solvent was removed from the filtrate *in vacuo* and the residue recrystallized from hexane to give $[Rh(cod)\{CH(PPh_2)$-$(P(S)Ph_2)$-*P,S*$\}]$ as yellow crystals (0.18 g, 0.29 mmol). Anal. Calcd. for $C_{33}H_{33}P_2RhS$: C, 63.3; H, 5.31. Found: C, 63.2; H, 5.35%.

Method B; A solution of $Li[CH(PPh_2)(P(S)Ph_2)]$ (0.43 g, 1.0 mmol) in tetrahydrofuran (5 ml) was added dropwise to a stirred solution of $[Rh_2Cl_2(cod)_2]$ (0.25 g, 0.51 mmol) in tetrahydrofuran (5 ml). After 3 h, the volume was reduced to about 2 ml by removal of solvent *in vacuo*, and $[Rh(cod)\{CH(PPh_2)(P(S)Ph_2)$-*P,S*$\}]$ was identified as the only product by ^{31}P NMR spectroscopy.

The following complexes of the general type $[M(cod)\{CH(PPh_2)(P(Y)R_2)$-*P,S*$\}]$, were prepared by procedures similar to that used for the example above. Both methods A and B were suitable for the sulphides but the selenide was obtained only by method A.

$[Ir(cod)\{CH(PPh_2)(P(S)Ph_2)$-*P,S*$\}]$. Yield: 52%. Anal. Calcd. for $C_{33}H_{33}P_2IrS$: C, 55.4; H, 4.65. Found: C, 55.6; H, 5.04%.

$[Ir(cod)\{CH(PPh_2)(P(S)^tBu_2)$-*P,S*$\}]$. Yield: 87%. Anal. Calcd. for $C_{29}H_{41}P_2IrS$: C, 51.5; H, 6.11. Found: C, 51.0; H, 6.07%.

$[Rh(cod)\{CH(PPh_2)(P(S)^tBu_2)$-*P,S*$\}]$. Recryst: diethyl ether. Yield: 82%. Anal. Calcd. for $C_{29}H_{41}P_2RhS$: C, 59.4; H, 7.05. Found: C, 59.9; H, 6.80%.

$[Rh(cod)\{CH(PPh_2)(P(Se)Ph_2)$-*P,Se*$\}]$. Yield: 90%. Anal. Calcd. for $C_{33}H_{33}P_2RhSe$: C, 58.9; H, 4.94. Found: C, 59.3; H, 5.19%. ^{77}Se NMR (C_6D_6): δ(Se) 196.3 ppm, ^1J(Se–P_B) 442 Hz, ^1J(Rh–Se) 27 Hz.

2.1.3. Protonation reactions

These were carried out on a small scale in 10 mm NMR tubes using approximately one molar equivalent of $HBF_4 \cdot Et_2O$ in either diethyl ether or tetrahydrofuran solution. Monitoring of the reactions by ^{31}P NMR spectroscopy indicated that all of the complexes, $[M(cod)\{CH(PPh_2)(P(S)R_2)_2$-*P,S*$\}]$, were rapidly converted in high yields to the corresponding cations, $[M(cod)\{CH_2(PPh_2)(P(S)R_2)_2$-*P,S*$\}]^+$.

2.1.4. $[Rh(CO)_2\{CH_2(PPh_2)(P(S)^tBu_2)\text{-}P,S\}]BF_4$

Carbon monoxide was bubbled through a stirred solution of $[Rh(cod)\{CH_2(PPh_2)(P(S)^tBu_2)\text{-}P,S\}]BF_4$ (0.75 g, 1.1 mmol) in dichloromethane (10 ml). After 7 h the solvent was removed *in vacuo* and the oily residue washed with hexane (3 × 20 ml) to remove free cod and leave $[Rh(CO)_2\{CH_2(PPh_2)(P(S)^tBu_2)\text{-}P,S\}]BF_4$ as a yellow powder (0.14 g, 0.23 mmol). Anal. Calcd. for $C_{23}H_{30}BF_4O_2P_2RhS$: C, 44.4; H, 4.86. Found: C, 44.8; H, 4.49%. Infrared (CH_2Cl_2): ν(CO) 2019s, 2082s, 1990w. ^{13}C NMR ($CDCl_3$): $\delta(CH_2)$ 27.7 ppm, δ(CO) *ca.* 182(m) ppm, $\delta(CMe_3)$ 38.7 ppm, $\delta(CH_3)$ 27.3 ppm, $^1J(P_A\text{–}CH_2)$ 25 Hz, $^1J(P_B\text{–}CH_2)$ 38 Hz, $^1J(P_B\text{–}CMe_3)$ 31 Hz.

2.1.5. $[Ir(CO)_2\{CH_2(PPh_2)(P(S)^tBu_2)\text{-}P,S\}]BF_4$

This complex was prepared by a procedure similar to the previous example above. Recryst: diethyl ether. Yield: 59%. Anal. Calcd. for $C_{23}H_{30}BF_4O_2P_2IrS$: C, 38.8; H, 4.25%. Found: C, 39.3; H, 4.62. Infrared (CH_2Cl_2): ν(CO) 2012s, 2079s, 1974w. ^{13}C NMR ($CDCl_3$): $\delta(CH_2)$ 26.1 ppm, δ(CO) *ca.* 174(m) ppm, $\delta(CMe_3)$ 38.8 ppm, $\delta(CH_3)$ 27.4 ppm, $^1J(P_A\text{–}CH_2)$ 31 Hz, $^1J(P_B\text{–}CH_2)$ 34 Hz, $^1J(P_B\text{–}CMe_3)$ 31 Hz.

2.1.6. $[Rh(CN^tBu)_2\{CH_2(PPh_2)(P(S)^tBu_2)\text{-}P,S\}BF_4$

Tertiary butylisocyanide (0.07 g, 0.84 mmol) was added dropwise to a stirred solution of $[Rh(cod)\{CH_2(PPh_2)(P(S)^tBu_2)\text{-}P,S\}]BF_4$ (0.10 g, 0.15 mmol) in dichloromethane (10 ml). After 72 h the solvent was removed *in vacuo* and the residue washed with diethyl ether (10 ml) and recrystallized from dichloromethane/hexane to give $[Rh(CN^tBu)_2\{CH_2(PPh_2)(P(S)^tBu_2)\text{-}P,S\}]BF_4 \cdot CH_2Cl_2$ as orange crystals (0.11 g, 0.14 mmol). Anal. Calcd. for $C_{32}H_{50}BCl_2F_4N_2P_2RhS$: C, 47.0; H, 6.17. Found: C, 46.9; H, 6.60%. ^{13}C NMR ($CDCl_3$): $\delta(CH_2)$ 30.0 ppm, δ, ($PCMe_3$) 38.1 ppm, $\delta(PCCH_3)$ 27.7 ppm, $^1J(P_A\text{–}CH_2)$ 17 Hz, $^1J(P_B\text{–}CH_2)$ 34 Hz, $^1J(P_B\text{–}CMe_3)$ 36 Hz, $\delta(CN)$ not obs., $\delta(NCMe_3)$ 58.4 ppm, $\delta(NCCH_3)$ 30.3 ppm, ^1J(N–C) 5 Hz.

2.1.7. $[Rh\{CH_2(PPh_2)_2\}\{CH_2(PPh_2)(P(S)^tBu_2)\text{-}P,S\}]BF_4$

A solution of $CH_2\{PPh_2\}_2$ (0.12 g, 0.31 mmol) in dichloromethane (5 ml) was added dropwise to a stirred solution of $[Rh(CO)_2\{CH_2(PPh_2)(P(S)^tBu_2)\text{-}P,S\}]BF_4$ (0.20 g, 0.32 mmol) in dichloromethane (10 ml). The solution immediately changed from yellow to orange and gas was evolved. After 30 min the solvent was removed *in vacuo* and the residue washed with diethyl ether (2 × 10 ml) and recrystallized from dichloromethane/hexane to give $[Rh\{CH_2(PPh_2)_2\}]\{CH_2(PPh_2)(P(S)^tBu_2)\text{-}P,S\}]BF_4$ as orange crystals (0.29 g, 0.31 mmol). Anal. Calcd. for $C_{46}H_{52}BF_4P_4RhS$: C, 58.1; H, 5.51. Found: C, 58.5; H, 5.33%.

2.1.8. $[Rh(cod)\{CH(SnMe_3)(PPh_2)(P(S)Ph_2)\text{-}P,S\}]Cl$

A solution of $SnClMe_3$ (0.06 g, 0.30 mmol) in benzene (5 ml) was added dropwise to a stirred solution of $[Rh(cod)\{CH(PPh_2)(P(S)Ph_2)\text{-}P,S\}]$ (0.19 g, 0.30 mmol) in benzene (10 ml). After 1 h, the solvent was removed *in vacuo* and the residue washed with hexane (2 × 10 ml) and recrystallized from tetrahydrofuran/diethyl ether to give $[Rh(cod)\{CH(SnMe_3)(PPh_2)(P(S)Ph_2)\text{-}P,S\}]Cl$ as an orange-brown powder (0.12 g, 0.15 mmol). Anal. Calcd. for $C_{36}H_{42}ClP_2RhSSn$: C, 52.4; H, 5.13; Cl, 4.3. Found: C, 52.9; H, 5.47; Cl, 4.9%.

2.1.9. $[RuCl_2(\eta^6\text{-}C_6H_6)\{CH_2(PPh_2)(P(S)Ph_2)\text{-}P\}]$

A solution of $CH_2\{PPh_2\}\{P(S)Ph_2\}$ (0.20 g, 0.48 mmol) in dichloromethane (5 ml) was added dropwise to a stirred solution of $[Ru_2Cl_4(\eta^6\text{-}C_6H_6)_2]$ (0.12 g, 0.24 mmol) in dichloromethane (5 ml). After 10 h the solution was filtered and the solvent was removed from the filtrate *in vacuo*. The residue was recrystallized from dichloromethane/diethyl ether to give $[RuCl_2(\eta^6\text{-}C_6H_6)\{CH_2(PPh_2)(P(S)Ph_2)\text{-}P\}]$ as orange-red crystals (0.28 g, 0.42 mmol). Anal. Calcd. for $C_{31}H_{28}Cl_2P_2RuS$: C, 55.9; H, 4.23; Cl, 10.6. Found: C, 55.8; H, 4.18; Cl, 10.6%. ^{13}C NMR ($CDCl_3$): $\delta(CH_2)$ 22.6 ppm, $\delta(C_6H_6)$ 88.4 ppm, $^1J(P_A\text{–}CH_2)$ 21 Hz, $^1J(P_B\text{–}CH_2)$ 49 Hz, $^1J(P_A\text{–}C_6H_6)$ 4 Hz.

2.1.10. $[RuCl_2(\eta^6\text{-}p\text{-}cymene)\{CH_2(PPh_2)(P(S)Ph_2)\text{-}P\}]$

This complex was prepared by a procedure similar to that for the benzene analogue above. Yield: 78% as dichloromethane solvate. Anal. Calcd. for $C_{36}H_{38}Cl_4P_2RuS$: C, 53.5; H, 4.74; Cl, 17.6. Found: C, 53.2; H, 4.72; Cl, 17.4%. ^{13}C NMR ($CDCl_3$): $\delta(CH_2)$ 22.2 ppm, δ(cymene) 17.2, 21.3, 30.0, 85.5, 94.1, 108.5 ppm, $^1J(P_A\text{–}CH_2)$ 20 Hz, $^1J(P_B\text{–}CH_2)$ 49 Hz.

2.1.11. $[RuCl(\eta^6\text{-}C_6H_6)\{CH_2(PPh_2)(P(S)Ph_2)\text{-}P,S\}]BF_4$

Silver tetrafluoroborate (0.021 g, 0.11 mmol) was added to a stirred solution of $[RuCl_2(\eta^6\text{-}C_6H_6)\{CH_2(PPh_2)(P(S)Ph_2)\text{-}P\}]$ (0.07 g, 0.11 mmol) in acetone (10 ml). After 2 h, stirring was discontinued, and the supernatant liquid decanted. Solvent was removed *in vacuo* from the orange supernatant and the resulting residue recrystallized from dichloromethane/diethyl ether to give $[RuCl(\eta^6\text{-}C_6H_6)\{CH_2(PPh_2)(P(S)Ph_2)\text{-}P,S\}]BF_4$ as orange crystals (0.07 g, 0.10 mmol). Anal. Calcd. for $C_{31}H_{28}BClF_4P_2RuS$: C, 51.9; H, 3.93; Cl, 4.9. Found: C, 51.5; H, 3.83; Cl, 5.6%. ^{13}C NMR

($CDCl_3$): $\delta(CH_2)$ 35.6 ppm, $\delta(C_6H_6)$ 90.5 ppm, $^1J(P_A-CH_2)$ 28 Hz, $^1J(P_B-CH_2)$ 52 Hz.

2.1.12. [RuCl(η⁶-p-cymene){CH(PPh₂)(P(S)Ph₂)-P,S}]

A solution of Li[CH(PPh₂){P(S)Ph₂}] (0.14 g, 0.33 mmol) in tetrahydrofuran (3 ml) was added to a stirred solution of $[Ru_2Cl_4(\eta^6\text{-}p\text{-cymene})_2]$ (0.10 g, 0.16 mmol) in tetrahydrofuran (5 ml). After 10 h, solvent was removed *in vacuo* and the brown residue was extracted with benzene. ^{31}P NMR spectroscopy of the extract showed that the product was primarily [RuCl(η⁶-*p*-cymene){CH(PPh₂)(P(S)Ph₂)-*P,S*}], but the instability of this product precluded isolation and purification.

2.2. X-Ray data collection

Compounds $[Ir(cod)\{CH_2(PPh_2)(P(S)^tBu_2)\text{-}P,S\}]BF_4 \cdot CHCl_3$, (**1**), $[Rh(cod)\{CH_2(PPh_2)(P(S)^tBu_2)\text{-}P,S\}]ClO_4 \cdot CH_2Cl_2$ (**2**), [Rh(cod){CH(PPh₂)(P(S)Ph₂)-*P,S*}] (**3**) and $[RuCl_2(p\text{-cymene})\{CH_2(PPh_2)(P(S)Ph_2)\text{-}P\}] \cdot CH_2Cl_2$ (**4**) were prepared as described above. Crystals of **2** and **4** suitable for study by X-ray diffraction were grown by vapour diffusion of diethyl ether into a solution of the complex in dichloromethane. Crystals of **1** were grown similarly from diethyl ether and chloroform and crystals of **3** were grown from hexane. Preliminary photographic work was carried out with Weissenberg and precession cameras using Cu Kα radiation. After establishment of symmetry and approximate unit cells the crystals were transferred to one of two diffractometers (Table 3) and the unit cells refined by least squares methods employing pairs of centring measurements. During the subsequent data collection there was no evidence of decomposition of any of the crystals.

The Picker 4-circle instrument was automated with a PDP 11/10 computer and used a $\theta/2\theta$ step scan with 144 (**1**) or 200 (**3**) steps of 0.01° in 2θ, counting for 0.25 s per step. Background measurements were for 18 (**1**) or 25 (**3**) s at each end of the scan. Each batch of 50 reflections was preceded by the measurement of three standard reflections, and, after application of Lorentz and polarization factors, each batch was scaled to maintain the sum of the standards constant. Absorption corrections were applied by a numerical integration using a Gaussian grid and with the crystal shape defined by perpendicular distances to crystal faces from a central origin.

Measurements on the CAD4 diffractometer used the NRCCAD modification of the Enraf-Nonius program [27], and the "Profile" $\omega/2\theta$ scan developed by Grant and Gabe [28]. Three standard reflections were measured every hour to check crystal stability and three others were measured every 400 reflections to check crystal orientation. Lorentz and polarization factors were applied but examination of the psi scans for **2** and

TABLE 3. Crystallographic data for compounds **1**–**4** **1**: $[Ir(cod)\{CH_2(PPh_2)(P(S)^tBu_2)\text{-}P,S\}]BF_4 \cdot CHCl_3$ **2**: $[Rh(cod)\{CH_2(PPh_2)(P(S)^tBu_2)\text{-}P,S\}]ClO_4 \cdot CH_2Cl_2$ **3**: [Rh(cod){CH(PPh₂)(P(S)Ph₂)-*P,S*}] **4**: $[RuCl_2(p\text{-cymene})\{CH_2(PPh_2)(P(S)Ph_2)\text{-}P\}] \cdot CH_2Cl_2$

	1	**2**	**3**	**4**
formula	$C_{30}H_{43}BCl_3F_4P_2SIr$	$C_{30}H_{44}Cl_3O_4P_2SRh$	$C_{33}H_{33}P_2SRh$	$C_{36}H_{38}Cl_4P_2SRu$
fw	883.06	771.85	626.54	807.59
space group	$P\bar{1}$ (No 2)	$P\bar{1}$ (No 2)	$P\bar{1}$ (No 2)	$P\bar{1}$ (No 2)
a, Å	12.307(7)	12.163(1)	10.650(4)	11.217(2)
b, Å	14.743(8)	14.564(1)	13.327(4)	17.124(3)
c, Å	10.877(6)	10.560(1)	10.419(3)	10.412(2)
α, deg	74.42(5)	77.69(1)	90.60(3)	90.58(1)
β, deg	107.65(6)	74.54(1)	102.64(3)	112.29(2)
γ, deg	105.47(5)	77.01(1)	83.15(3)	97.53(1)
V, Å³	1774	1733	1432	1831
Z	2	2	2	2
diffractometer	Picker 4-circle	Enraf-Nonius CAD4	Picker 4-circle	Enraf-Nonius CAD4
radiation (λ, Å)	Mo Kα(0.71069)	Mo Kα(0.71069)	Mo Kα(0.71069)	Mo Kα(0.71069)
μ, cm^{-1}	41.77	8.98	7.84	8.76
transm factor range	0.39–0.56		0.72–0.89	
temperature, K	295	295	295	295
no of obs reflcns ($I > 3.0\,\sigma(I)$)	5243	3966	5045	5675
parameters refined	379	356	299	412
R	0.067	0.057	0.062	0.041
R_w	0.088	0.090	0.073	0.061

$w = 1/(\sigma^2(F) + 0.001F^2)$; $\Delta = ||F_o| - |F_c||$. $R = (\Sigma\Delta/\Sigma F_o)$; $R_w = (\Sigma w\Delta^2/\Sigma wF_o^2)^{1/2}$

4 indicated that absorption corrections were unnecessary.

2.3. Structure solution and refinement

Structures **1**, **3** and **4** were found and refined using the SHELX-76 program package [29], and structure **2** using the NRCVAX program [30]. Illustrations were drawn using ORTEP [31]. The atomic scattering factors used were for neutral atoms, with corrections for anomalous dispersion [32]. The structures were solved by direct methods, developed by standard Fourier synthesis procedures using difference maps, and refined by the method of least squares minimising $\Sigma w\Delta^2$ where $\Delta = \| F_o | - | F_c \|$. The weights were obtained from counting statistics using $w = 1/(\sigma^2(F) + 0.001F^2)$. All non-hydrogen atoms were treated anisotropically except for the solvent molecule in structure **2** and the cod ligand, C(1)–C(8), in structure **3**. In structures **1** and **2**, no hydrogen atoms were located and none were included in the refinement. In structures **3** and **4**, the only hydrogen atoms to be located were those attached to C(10). Other hydrogen atoms in **3** and **4** were included in the refinement but were assigned group temperature factors and allowed to ride on their respective carbon atoms. The final difference maps gave no indication that any material had been overlooked.

3. Results

3.1. Synthesis

The ligands, $CH_2(PPh_2)(P(Y)R_2)$, Y = S or Se, R = Ph or ^{t}Bu react smoothly under mild conditions with the chloro-bridged complexes, $[M_2Cl_2(cod)_2]$, M = Rh or Ir, to yield cations, $[M(cod)\{CH_2(PPh_2)(P(Y)R_2)$-*P,S*$\}]^+$. In order to provide a counter ion, and also to facilitate the reaction by precipitation of NaCl, the reactions are carried out in acetone in the presence of $NaClO_4$ or $NaBF_4$. In the case of one selenium complex (R = Ph, M = Ir), we also inadvertently prepared the monoseleno cation by the reaction of $CH_2(P(Se)Ph_2)_2$ with $[Ir_2Cl_2(cod)_2]$. Evidently the initial diseleno complex is unstable and spontaneously ejects one atom of selenium. Reactions of the monocations, $[M(cod)\{CH_2(PPh_2)(P(Y)R_2)$-*P,S*$\}]^+$, with sodium hydride in tetrahydrofuran result in facile deprotonation to form the neutral complexes, $[M(cod)\{CH(PPh_2)(P(Y)R_2)$-*P,S*$\}]$, and when Y = S, these products are also accessible *via* reactions of $[M_2Cl_2(cod)_2]$ with $Li[CH(PPh_2)(P(S)R_2)]$. The deprotonation by sodium hydride demonstrates the enhanced acidity of the coordinated ligands since the free ligands are not deprotonated under similar conditions. Moreover, since reactions of the neutral complexes, $[M(cod)\{CH(PPh_2)(P(S)R_2)$-*P,S*$\}]$, with HBF_4 result in immediate reprotonation with reformation of the cations, $[M(cod)\{CH_2(PPh_2)(P(Y)R_2)$-*P,S*$\}]^+$, the sequence provides an important confirmation of the assigned structures. Reactivity of the methine carbons is also demonstrated by the reaction of $[Rh(cod)\{CH(PPh_2)(P(S)Ph_2)$-*P,S*$\}]$ with $SnClMe_3$ to form $[Rh(cod)\{CH(SnMe_3)(PPh_2)(P(S)Ph_2)$-*P,S*$\}]Cl$.

We were unable to obtain any evidence for coordination *via* carbon of the anions, $[CH(PPh_2)(P(S)R_2)]^-$. This is similar to our previous results with platinum and palladium complexes of these ligands [9], and to results with rhodium and iridium complexes of the $[CH(P(S)Ph_2)_2]^-$ anion [33]. Overall these results are a considerable contrast with platinum complexes of $[CH(P(S)Ph_2)_2]^-$ since these are frequently bonded *via* carbon [18].

The cod ligands in the cations, $[M(cod)\{CH_2(PPh_2)(P(S)^tBu_2)$-*P,S*$\}]^+$, are relatively labile and reactions under mild conditions with other ligands, Lg = $(CO)_2$, $(CN^tBu)_2$, or dppm, result in displacement of cod to form $[M(Lg)\{CH_2(PPh_2)(P(S)^tBu_2)$-*P,S*$\}]^+$.

Reactions of the chloro-bridged ruthenium dimers, $[Ru_2Cl_4L_2]$, L = η^6-benzene or η^6-*p*-cymene, with $CH_2(PPh_2)(P(S)Ph_2)$ are similar to the above rhodium and iridium chemistry except that chloride is not displaced even when $NaBF_4$ or $NaClO_4$ are added to the reaction mixtures. The resulting complexes, $[RuCl_2L\{CH_2(PPh_2)(P(S)Ph_2)$-*P*$\}]$, contain monodentate phosphorus sulphide ligands. These results are consistent with a previously reported bridge cleavage reaction using $CH_2(PPh_2)_2$ to yield $[RuCl_2L\{CH_2(PPh_2)_2$-*P*$\}]$ [34]. Removal of chloride from our complexes requires a subsequent reaction with $AgClO_4$ to yield chelate complexes, $[RuClL\{CH_2(PPh_2)(P(S)Ph_2)$-*P,S*$\}]ClO_4$. Reaction of $[Ru_2Cl_4(\eta^6$-*p*-cymene$)_2]$ with $Li[CH(PPh_2)(P(S)Ph_2)]$ differs from the reaction with the neutral ligand in that chloride is displaced with direct formation of the chelate complex, $[RuClL\{CH(PPh_2)(P(S)$-$Ph_2)$-*P,S*$\}]$.

3.2. NMR Spectroscopy

Data derived from ^{31}P and selected ^{13}C NMR spectra are collected in Tables 1 and 2. Other ^{13}C and also ^{77}Se data are included in the Experimental section. The labelling scheme used is shown in Scheme 2.

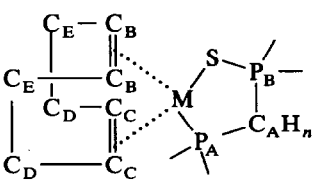

Scheme 2. Atom labels for NMR parameters.

For the rhodium/cyclooctadiene complexes shown in Table 1, the ^{31}P spectra each consist of two resonances, both doubled by P–P coupling, and with the upfield resonance also doubled by coupling to rhodium. Thus, the upfield resonance is assigned to P_A, directly bonded to rhodium, and since the spectra of iridium/cyclooctadiene complexes are similar, but of course lack the Rh–P coupling, their assignment is equally straightforward. The only more complex ^{31}P spectrum is that of the bis(diphenylphosphino)methane substitution product, which consists of 4 resonances, each displaying an essentially first order pattern with 16 lines (a doublet of doublets of doublets of doublets) arising from coupling to three chemically shifted phosphorus atoms and a rhodium.

^{31}P NMR spectra of the ruthenium complexes each consist of two doublet resonances, one of which (Table 1) is very close in chemical shift to the coordinated

TABLE 4. Fractional atomic coordinates and temperature parameters for compound 1, $[Ir(cod)\{CH_2(PPh_2)(P(S)^tBu_2)\}]BF_4 \cdot CHCl_3$

Atom	x	y	z	U_{eq}
Ir(1)	23268(4)	11951(3)	−14036(4)	410(2)
S(1)	1335(4)	1494(2)	−92(4)	69(2)
P(1)	2194(3)	2768(2)	443(3)	47(1)
P(2)	3017(3)	2804(2)	−1956(3)	39(1)
C(1)	2622(12)	990(10)	−3143(13)	61(6)
C(2)	3515(12)	713(9)	−1997(15)	63(6)
C(3)	3638(15)	−327(10)	−1382(19)	84(8)
C(4)	2996(18)	−788(10)	−331(18)	90(9)
C(5)	1948(13)	−367(8)	−500(14)	64(6)
C(6)	1112(14)	−202(9)	−1580(14)	73(7)
C(7)	1069(15)	−478(11)	−2875(15)	82(7)
C(8)	1591(15)	329(11)	−3830(14)	81(7)
C(10)	3157(11)	3440(8)	−626(11)	49(5)
C(11)	2064(11)	3388(8)	−3406(10)	48(5)
C(12)	2264(13)	4416(9)	−3790(13)	65(6)
C(13)	1553(15)	4843(11)	−4893(14)	74(7)
C(14)	610(17)	4267(12)	−5627(13)	79(8)
C(15)	384(14)	3296(12)	4720(14)	79(7)
C(16)	1126(13)	2825(10)	−4135(12)	64(6)
C(21)	4457(10)	3231(7)	−2300(10)	43(4)
C(22)	5420(11)	3081(9)	−1275(12)	56(5)
C(23)	6529(13)	3367(10)	−1479(14)	68(6)
C(24)	6697(15)	3838(10)	−2744(17)	76(7)
C(25)	5712(15)	3950(11)	−3810(16)	76(7)
C(26)	4581(12)	3644(9)	−3580(12)	60(5)
C(31)	1073(12)	3471(8)	217(14)	58(5)
C(32)	550(15)	3736(12)	−1284(15)	83(8)
C(33)	118(14)	2872(11)	942(19)	84(8)
C(34)	1637(17)	4396(11)	798(17)	88(9)
C(35)	3189(15)	2551(13)	2144(13)	82(8)
C(36)	3971(17)	3492(16)	2512(17)	103(10)
C(37)	3913(17)	1835(15)	2136(16)	105(10)
C(38)	2417(19)	2013(19)	3141(16)	130(12)
B(1)	−2843(16)	3417(12)	2191(16)	69(7)
F(1)	−3506(10)	4044(7)	1415(10)	106(6)
F(2)	−3217(14)	2590(7)	1851(12)	145(8)
F(3)	−2772(14)	3301(9)	3491(10)	140(7)
F(4)	−1802(13)	3844(12)	2002(15)	166(9)
C(0)	−2831(30)	1531(15)	−4213(21)	145(16)
Cl(1)	−4134(12)	1440(9)	−3587(11)	235(9)
Cl(2)	−3522(14)	558(8)	5012(13)	258(10)
Cl(3)	−1658(11)	1431(14)	−3210(12)	411(13)

Estimated standard deviations are given in parentheses. Coordinates $\times 10^n$ where $n = 5$ for Ir, and 4 otherwise. Temperature parameters $\times 10^n$ where $n = 4$ for Ir, and 3 otherwise. U_{eq} = equivalent isotropic temperature parameter = $1/3\ \Sigma_i\Sigma_j U_{ij} a_i^* a_j^* (\mathbf{a}_i \cdot \mathbf{a}_j)$.

TABLE 5. Fractional atomic coordinates and temperature parameters for compound 2, $[Rh(cod)\{CH_2(PPh_2)(P(S)^tBu_2)\}]ClO_4 \cdot CH_2Cl_2$

Atom	x	y	z	U_{eq}
Rh(1)	26561(4)	10798(3)	34261(5)	304(4)
S(1)	38635(16)	14678(13)	45623(20)	452(11)
P(1)	29746(15)	26727(12)	52815(17)	334(10)
P(2)	20084(14)	26744(11)	29124(16)	290(9)
C(1)	2127(7)	0816(5)	1793(7)	46(1)
C(2)	1315(7)	0579(5)	2938(8)	47(1)
C(3)	1199(8)	−0447(6)	3635(10)	61(1)
C(4)	1916(8)	−0843(6)	4644(10)	65(1)
C(5)	3025(7)	−0450(5)	4383(8)	47(1)
C(6)	3777(7)	−0342(5)	3199(8)	49(1)
C(7)	3697(8)	−0663(6)	1940(9)	62(1)
C(8)	3087(10)	0151(7)	1029(9)	72(1)
C(10)	1945(6)	3319(5)	4281(6)	33(1)
C(11)	2998(6)	3221(4)	1490(6)	32(1)
C(12)	2816(7)	4208(5)	1088(7)	44(1)
C(13)	3607(7)	4631(6)	0014(8)	52(1)
C(14)	4556(8)	4027(6)	−0673(8)	56(1)
C(15)	4727(8)	3077(7)	−0287(8)	58(1)
C(16)	3936(6)	2649(5)	0804(7)	43(1)
C(21)	0580(6)	3115(4)	2561(7)	34(1)
C(22)	−0385(6)	3045(5)	3600(7)	46(1)
C(23)	−1497(7)	3371(6)	3371(9)	57(1)
C(24)	−1626(8)	3785(7)	2077(10)	66(1)
C(25)	−0673(7)	3826(7)	1034(9)	63(1)
C(26)	0440(7)	3490(6)	1274(7)	47(1)
C(31)	4035(6)	3451(5)	5141(8)	44(1)
C(32)	3471(9)	4362(7)	5745(10)	71(1)
C(33)	4557(8)	3732(7)	3644(9)	63(1)
C(34)	5025(8)	2891(7)	5813(11)	74(1)
C(35)	2090(7)	2361(7)	6991(7)	57(1)
C(36)	1311(9)	3209(9)	7543(10)	80(1)
C(37)	1287(10)	1681(8)	6873(10)	80(1)
C(38)	2895(12)	1792(13)	7909(11)	131(1)
Cl(1)	7991(2)	3510(2)	7249(2)	51(1)
O(1)	8416(11)	2616(6)	6958(12)	151(1)
O(2)	6927(8)	3906(11)	6964(10)	162(1)
O(3)	7886(9)	3510(6)	8595(7)	110(1)
O(4)	8745(9)	4126(7)	6385(9)	127(1)
C(0)	7844(16)	1784(14)	0877(19)	143(1)′
Cl(2)	6741(5)	1359(4)	1907(5)	152(2)′
Cl(3)	9162(7)	0923(6)	0917(8)	219(3)′

Estimated standard deviations are given in parentheses. Coordinates $\times 10^n$ where $n = 5$ for Rh, S, P and 4 otherwise. Temperature parameters $\times 10^n$ where $n = 4$ for Rh, S, P and 3 otherwise. U_{eq} = equivalent isotropic temperature parameter = $1/3\ \Sigma_i\Sigma_j U_{ij} a_i^* a_j^* (\mathbf{a}_i \cdot \mathbf{a}_j)$, primed values indicate that U_{iso} is given. $T = \exp -(8\pi^2 U_{iso} \sin^2\theta/\lambda^2)$.

phosphorus (−115.5 ppm) of the known complex, $[RuCl_2L\{CH_2(PPh_2)_2\text{-}P\}]$ [34].

3.3. X-Ray crystal structures

The atom labelling schemes and structures of single cations of compounds $[Ir(cod)\{CH_2(PPh_2)(P(S)^tBu_2)\text{-}P,S\}]BF_4 \cdot CHCl_3$ (**1**), $[Rh(cod)\{CH_2(PPh_2)(P(S)^tBu_2)\text{-}P,S\}]ClO_4 \cdot CH_2Cl_2$ (**2**), $[Rh(cod)\{CH(PPh_2)(P(S)Ph_2)\text{-}P,S\}]$ (**3**) and $[RuCl_2(p\text{-cymene})\{CH_2(PPh_2)(P(S)Ph_2)\text{-}P\}] \cdot CH_2Cl_2$ (**4**) are shown in Figs. 1–4. Unit cell and other parameters related to the crystal structure determinations are in Table 3. Fractional atomic coordinates and isotropic temperature parameters are given in Tables 4–7, and the most significant bond lengths and angles are collected in Tables 8 and 9 [35*].

TABLE 6. Fractional atomic coordinates and temperature parameters for compound **3**, $[Rh(cod)\{CH_2(PPh_2)(P(S)Ph_2)\}]$

Atom	x	y	z	U_{eq}
Rh	−33105(3)	18289(3)	14934(3)	332(1)
S(1)	−54964(11)	17523(9)	15156(12)	392(4)
P(1)	−58061(11)	25077(9)	31536(11)	329(4)
P(2)	−32481(11)	30415(8)	30909(11)	317(4)
C(1)	−1294(5)	1347(4)	1952(5)	46(1)′
C(2)	−1513(5)	2133(4)	1054(5)	51(1)′
C(3)	−1507(7)	2009(5)	−402(6)	70(2)′
C(4)	−2791(8)	1755(6)	−1246(8)	85(2)′
C(5)	−3641(6)	1253(5)	−512(6)	57(1)′
C(6)	−3281(6)	439(5)	267(6)	60(1)′
C(7)	−1937(7)	−157(6)	524(7)	75(2)′
C(8)	−999(6)	247(5)	1673(6)	64(2)′
C(10)	−4433(5)	2969(4)	3970(5)	38(2)
C(11)	−3368(5)	4325(3)	2395(5)	38(2)
C(12)	−3330(6)	4488(5)	1103(5)	55(2)
C(13)	−3458(7)	5474(5)	614(7)	71(3)
C(14)	−3619(6)	6282(5)	1395(7)	70(3)
C(15)	−3696(7)	6126(5)	2667(7)	69(3)
C(16)	−3559(6)	5153(4)	3167(6)	58(2)
C(21)	−1735(4)	2980(3)	4342(4)	35(1)
C(22)	−1551(5)	2310(4)	5393(5)	44(2)
C(23)	−399(6)	2203(5)	6329(6)	57(2)
C(24)	590(6)	2753(5)	6219(6)	64(2)
C(25)	425(5)	3407(5)	5170(6)	62(2)
C(26)	−737(5)	3527(4)	4241(5)	49(2)
C(31)	−7174(5)	3483(4)	2627(5)	40(2)
C(32)	−8295(5)	3315(4)	1701(6)	55(2)
C(33)	−9311(6)	4100(5)	1360(7)	66(2)
C(34)	−9208(7)	5034(5)	1934(7)	74(3)
C(35)	−8121(7)	5193(5)	2797(7)	75(3)
C(36)	−7079(6)	4433(4)	3148(5)	57(2)
C(41)	−6373(4)	1649(3)	4200(5)	37(2)
C(42)	−7534(6)	1234(5)	3784(7)	64(2)
C(43)	−7859(6)	513(5)	4555(7)	70(3)
C(44)	−7070(6)	203(4)	5729(6)	58(2)
C(45)	−5917(6)	618(4)	6171(5)	56(2)
C(46)	−5579(5)	1351(4)	5397(5)	49(2)

Estimated standard deviations are given in parentheses. Coordinates $\times 10^n$ where $n = 5$ for Rh, S, P and 4 for C. Temperature parameters $\times 10^n$ where $n = 4$ for Rh, S, P and 3 for C. U_{eq} = equivalent isotropic temperature parameter $= 1/3\ \Sigma_i\Sigma_j U_{ij} a_i^* a_j^* (\mathbf{a}_i \cdot \mathbf{a}_j)$, primed values indicate that U_{iso} is given. $T = \exp -(8\pi^2 U_{iso} \sin^2\theta/\lambda^2)$.

TABLE 7. Fractional atomic coordinates and temperature parameters for compound **4**, $[RuCl_2(p\text{-cymene})\{CH_2(PPh_2)(P(S)Ph_2)\}] \cdot CH_2Cl_2$

Atom	x	y	z	U_{eq}
Ru(1)	−10270(3)	10992(1)	12880(3)	310(1)
S(1)	7439(10)	46625(6)	31893(12)	498(4)
P(1)	16881(9)	37829(5)	38969(10)	358(3)
P(2)	−6808(8)	23784(5)	23439(8)	279(3)
Cl(1)	10382(9)	8918(6)	30521(10)	446(4)
Cl(2)	1669(9)	17248(6)	−147(9)	435(4)
C(1)	−2019(4)	71(2)	1968(4)	47(2)
C(2)	−2793(4)	688(2)	1670(4)	43(1)
C(3)	−3151(4)	1020(2)	364(4)	42(1)
C(4)	−2754(4)	750(2)	−674(4)	44(1)
C(5)	−1974(4)	124(2)	−360(4)	50(2)
C(6)	−1626(4)	−206(2)	918(5)	49(2)
C(7)	−1638(5)	−305(3)	3342(5)	67(2)
C(10)	1020(3)	2845(2)	2871(4)	33(1)
C(11)	−1662(3)	3042(2)	1188(3)	34(1)
C(12)	−1243(4)	3452(2)	252(4)	47(2)
C(13)	−2051(5)	3906(3)	−706(4)	61(2)
C(14)	−3294(5)	3916(3)	−785(5)	67(2)
C(15)	−3731(5)	3511(3)	127(5)	60(2)
C(16)	−2929(4)	3075(2)	1116(4)	42(1)
C(21)	−983(3)	2433(2)	3933(3)	32(1)
C(22)	−1227(3)	3129(2)	4437(4)	36(1)
C(23)	−1292(4)	3166(2)	5745(4)	45(2)
C(24)	−1140(4)	2522(3)	6538(4)	52(2)
C(25)	−911(5)	1822(3)	6037(4)	56(2)
C(26)	−823(4)	1782(2)	4749(4)	44(2)
C(31)	3303(4)	3929(2)	3853(5)	45(2)
C(32)	4416(4)	3839(3)	4985(6)	70(2)
C(33)	5623(5)	3953(4)	4885(8)	95(3)
C(34)	5716(5)	4151(3)	3686(8)	88(3)
C(35)	4630(6)	4252(3)	2527(7)	79(3)
C(36)	3411(5)	4141(3)	2610(6)	61(2)
C(41)	1944(4)	3603(2)	5693(4)	44(1)
C(42)	1808(4)	4211(3)	6515(5)	57(2)
C(43)	2032(5)	4097(4)	7907(5)	78(2)
C(44)	2384(6)	3400(5)	8460(5)	91(3)
C(45)	2480(7)	2788(4)	7636(5)	92(3)
C(46)	2272(5)	2903(3)	6268(5)	68(2)
C(51)	−3157(5)	1070(3)	−2097(4)	58(2)
C(52)	−4052(8)	418(4)	−3171(6)	118(4)
C(53)	−3754(6)	1816(3)	−2231(5)	85(3)
C(0)	3847(6)	1937(4)	2370(8)	94(3)
Cl(3)	5307(3)	1818(1)	3724(2)	148(1)
Cl(4)	4047(2)	1781(1)	8025(2)	113(1)

Estimated standard deviations are given in parentheses. Coordinates $\times 10^n$ where $n = 5$ for Ru, S, P, Cl(1) and Cl(2), and 4 otherwise. Temperature parameters $\times 10^n$ where n = Ru, S, P, Cl(1) and Cl(2), and 3 otherwise. U_{eq} = equivalent isotropic temperature parameter $= 1/3\ \Sigma_i\Sigma_j U_{ij} a_i^* a_j^* (\mathbf{a}_i \cdot \mathbf{a}_j)$.

In structures **1–3**, the metal coordination is approximately square planar, with two positions occupied by

* Reference number with asterisk refers to a note in the list of references.

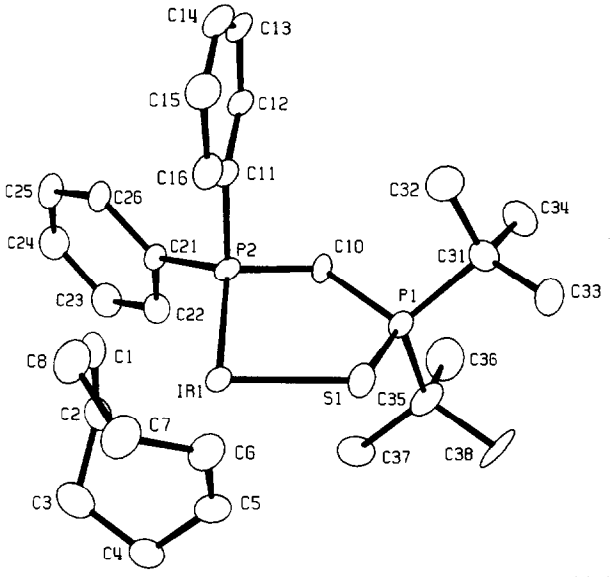

Fig. 1. ORTEP plot for a single cation of $[Ir(cod)\{CH_2(PPh_2)(P(S)^tBu_2)\text{-}P,S\}]BF_4 \cdot CHCl_3$, (1)

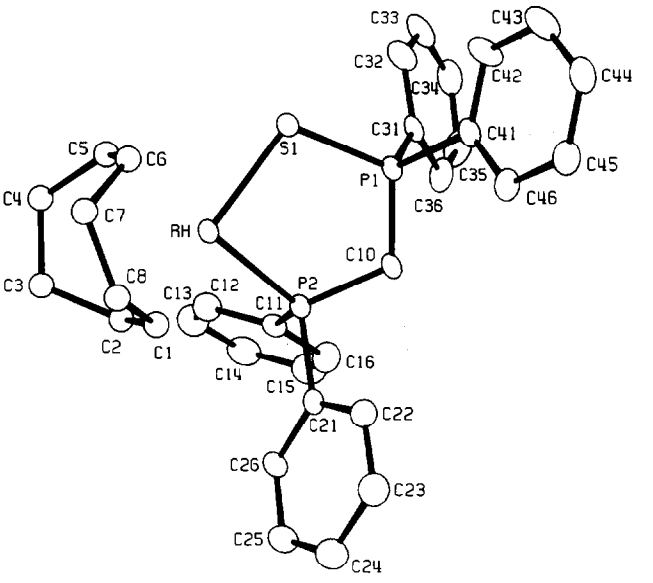

Fig. 3. ORTEP plot for a single molecule of $[Rh(cod)\{CH(PPh_2)(P(S)Ph_2)\text{-}P,S\}]$, (3)

the double bonds of a chelating cyclooctadiene ligand, and the coordination completed by a $[CH_n(PPh_2)(P(S)R_2)]^{(2-n)-}$ ligand coordinated *via* phosphorus and the S atom so as to form a 5-member chelate ring. The interbond angles are closely similar in all three structures, with the narrow angle between the cod double bonds (DB), 85.8–86.7°, compensated mainly by a wide DB–M–P angle, 94.5–94.8°. The other angles are close to 90°: DB–M–S, 90.1–90.9°; and P–M–S, 87.5–89.2°.

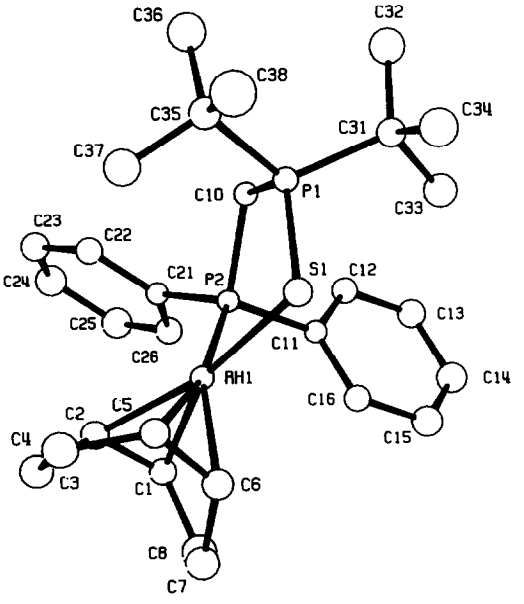

Fig. 2. ORTEP plot for a single cation of $[Rh(cod)\{CH_2(PPh_2)(P(S)^tBu_2)\text{-}P,S\}]ClO_4 \cdot CH_2Cl_2$, (2)

The bond lengths, M–P (2.28–2.30 Å) and M–S (2.32–2.35 Å) are closely similar to those observed previously in *trans*-$[PtCl(PEt_3)\{CH_2(PPh_2)(P(S)^tBu_2)\text{-}P,S\}]ClO_4$

TABLE 8. Selected interatomic distances for compounds **1–4** **1**: $[Ir(cod)\{CH_2(PPh_2)(P(S)^tBu_2)\text{-}P,S\}]BF_4 \cdot CHCl_3$ **2**: $[Rh(cod)\{CH_2(PPh_2)(P(S)^tBu_2)\text{-}P,S\}]ClO_4 \cdot CH_2Cl_2$ **3**: $[Rh(cod)\{CH(PPh_2)(P(S)Ph_2)\text{-}P,S\}]$ **4**: $[RuCl_2(p\text{-cymene})\{CH_2(PPh_2)(P(S)Ph_2)\text{-}P\}] \cdot CH_2Cl_2$

	1	2	3		4
M(1)–S(1)	2.324(3)	2.349(2)	2.346(1)	Ru(1)–Cl(2)	2.422(1)
				Ru(1)–Cl(2)	2.411(1)
M(1)–P(2)	2.275(3)	2.275(2)	2.304(1)	Ru(1)–P(2)	2.359(1)
M(1)–C(1)	2.141(12)	2.127(7)	2.115(5)	Ru(1)–C(1)	2.225(4)
M(1)–C(2)	2.106(13)	2.145(7)	2.146(6)	Ru(1)–C(2)	2.195(4)
M(1)–C(5)	2.231(11)	2.241(7)	2.188(6)	Ru(1)–C(3)	2.189(4)
M(1)–C(6)	2.216(12)	2.230(7)	2.240(6)	Ru(1)–C(4)	2.226(3)
				Ru(1)–C(5)	2.227(4)
				Ru(1)–C(6)	2.233(4)
S(1)–P(1)	2.034(5)	2.026(3)	2.041(2)	S(1)–P(1)	1.945(1)
P(1)–C(10)	1.824(10)	1.823(6)	1.702(5)	P(1)–C(10)	1.823(3)
P(1)–C(31)	1.859(12)	1.858(7)	1.823(5)	P(1)–C(31)	1.814(4)
P(1)–C(35)	1.883(15)	1.860(8)	1.828(5) [a]	P(1)–C(41)	1.817(4)
P(2)–C(10)	1.870(11)	1.861(6)	1.724(5)	P(2)–C(10)	1.838(4)
P(2)–C(11)	1.814(11)	1.816(6)	1.844(5)	P(2)–C(11)	1.817(3)
P(2)–C(21)	1.832(11)	1.819(7)	1.830(5)	P(2)–C(21)	1.815(4)
C(1)–C(2)	1.437(20)	1.377(12)	1.376(7)	C(1)–C(2)	1.419(6)
C(1)–C(8)	1.508(20)	1.508(12)	1.502(8)	C(1)–C(6)	1.422(7)
C(2)–C(3)	1.527(19)	1.538(11)	1.525(8)	C(2)–C(3)	1.412(6)
C(3)–C(4)	1.495(23)	1.494(13)	1.527(9)	C(3)–C(4)	1.411(7)
C(4)–C(5)	1.518(22)	1.519(12)	1.520(9)	C(4)–C(5)	1.434(6)
C(5)–C(6)	1.321(21)	1.340(12)	1.329(8)	C(5)–C(6)	1.386(6)
C(6)–C(7)	1.551(19)	1.532(12)	1.520(9)		
C(7)–C(8)	1.497(21)	1.542(14)	1.521(9)		

[a] P(1)–C(41)

(Pt–P 2.30 Å, Pt–S 2.28 Å) [9] and $[Au(C_6F_5)_2\{CH(PPh_2)(P(S)Ph_2)$-*P*,*S*$\}]$ (Au–P 2.33 Å, Au–S 2.35 Å) [13].

The chelate ligands, $CH_2\{PPh_2\}\{P(S)^tBu_2\}$, in structures **1** and **2**, have a planar backbone consisting of the P, C, P, and S atoms, and the metal atoms lie almost 1 Å out of this plane. Thus in **1**, χ^2 is 19.02 for the P, C, P, S plane, all four atoms lie within 0.05 Å of the best plane, and the iridium is 0.73 Å from the plane. Corresponding figures for **2** are 1.63 and 0.01 Å, and the rhodium is 0.94 Å from the ligand plane. This contrasts somewhat with the ligand conformation in **3**, where the ligand backbone is puckered, presumably to accommodate some rehybridization at the central carbon atom, and no simple planar description is appropriate. Considering the plane formed by the P, P, and S atoms, the carbon and rhodium atoms are respectively 0.24 and 0.42 Å out of plane, both on the same side.

The P–S bond lengths (2.03–2.04 Å) in structures **1–3** are similar to those in *trans*-$[PtCl(PEt_3)\{CH_2(PPh_2)(P(S)^tBu_2)$-*P*,*S*$\}]ClO_4$ (2.05 Å [9]) and $[Au(C_6F_5)_2\{CH(PPh_2)(P(S)Ph_2)$-*P*,*S*$\}]$ (2.06 Å [13]). Essentially the only significant difference between the structures **1–3** is the shortening of the ligand backbone P–C bonds in the deprotonated ligand of **3**. Thus C(10)–P(1) shortens from 1.82 Å in **1**/**2** to 1.70 Å in **3**. Corresponding data for C(10)–P(2) are 1.87 to 1.72 Å and similar changes occur between the protonated ligand of *trans*-$[PtCl(PEt_3)\{CH_2(PPh_2)(P(S)^tBu_2)$-*P*,*S*$\}]ClO_4$ (P–C lengths 1.83, 1.86 Å [9]) and the deprotonated ligand of $[Au(C_6F_5)_2\{CH(PPh_2)(P(S)Ph_2)$-*P*,*S*$\}]$ (P–C lengths 1.70, 1.72 Å [13]).

Structure **4** is completely different, since it contains a monodentate $CH_2(PPh_2)(P(S)Ph_2)$ ligand, coordinated only *via* phosphorus. This phosphorus atom and two chloride ligands occupy approximately octahedral coordination positions around the ruthenium, although the inter-ligand angles (Table 9) are significantly less than 90°. Coordination about the ruthenium is completed by an η^6-*p*-cymene ligand. Within the phosphine sulphide ligand the P–C(10) lengths (1.82, 1.84 Å) are similar to those in **1** and **2**, and the known platinum complex [9]. The P–S bond (1.95 Å) is slightly shorter than those in the other complexes, as would be expected if the P–S bond is weakened slightly by coordination.

4. Discussion

The ^{31}P NMR results in Table 1 show that coordination of the $[CH_2(PPh_2)(P(S)Ph_2)]$ ligand induces two main changes, namely pronounced deshielding of the directly coordinated phosphorus (P_A) and a sharp reduction in the P–P coupling constant. Basically, these effects are similar to those observed previously in platinum and palladium complexes of this ligand [9], and they are also observed in the other ligands included in the present study. For simplicity, the present discussion will focus on the $CH_2(PPh_2)(P(S)Ph_2)$ ligand but the comments apply equally to the other ligands in the study.

The coordination shift for P_A in $[Rh(cod)\{CH_2(PPh_2)(P(S)Ph_2)$-*P*,*S*$\}]^+$ is +68.1 ppm. For the corresponding Ir complex the value is +58.0 ppm. Coordi-

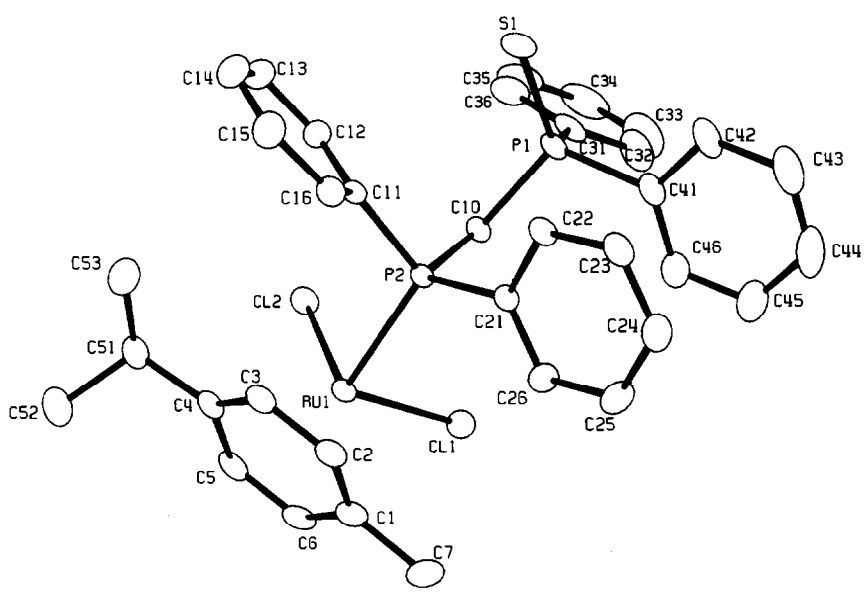

Fig. 4. ORTEP plot for a single molecule of $[RuCl_2(p\text{-cymene})\{CH_2(PPh_2)(P(S)\text{-}Ph_2)$-*P*$\}]\cdot CH_2Cl_2$, (**4**)

TABLE 9. Selected bond angles for compounds 1–4 1: [Ir(cod){$CH_2(PPh_2)$(P(S)$^tBu_2$)-*P,S*}]$BF_4 \cdot CHCl_3$ 2: [Rh(cod){$CH_2(PPh_2)$(P(S)$^tBu_2$)-*P,S*}]$ClO_4 \cdot CH_2Cl_2$ 3: [Rh(cod){$CH(PPh_2)$(P(S)Ph_2)-*P,S*}] 4: [$RuCl_2$(*p*-cymene){$CH_2(PPh_2)$(P(S)Ph_2)-*P*}] $\cdot CH_2Cl_2$

	1	2	3		4
S(1)–M(1)–P(2)	89.2(1)	87.5(1)	88.7(1)	P(2)–Ru(1)–Cl(1)	87.8(1)
S(1)–M(1)–C(1)	158.0(4)	157.9(2)	155.9(1)	P(2)–Ru(1)–Cl(2)	84.0(1)
S(1)–M(1)–C(2)	161.6(4)	164.1(2)	165.8(1)	Cl(1)–Ru(1)–Cl(2)	88.0(1)
S(1)–M(1)–C(5)	89.3(4)	89.7(2)	90.0(2)	C1–6–Ru(1)–P(2) [a]	131.4
S(1)–M(1)–C(6)	91.0(4)	92.0(2)	90.6(2)	C1–6–Ru(1)–Cl(1) [a]	125.2
P(2)–M(1)–C(1)	90.4(4)	90.9(2)	95.6(1)	C1–6–Ru(1)–Cl(2) [a]	126.4
P(2)–M(1)–C(2)	98.2(3)	98.0(2)	93.4(1)		
P(2)–M(1)–C(5)	168.4(4)	167.0(2)	156.1(2)		
P(2)–M(1)–C(6)	157.0(4)	157.9(2)	169.0(2)		
C(1)–M(1)–C(2)	39.5(5)	37.6(3)	37.7(2)		
C(1)–M(1)–C(5)	95.2(5)	96.5(3)	95.2(2)		
C(1)–M(1)–C(6)	80.9(5)	81.4(3)	80.7(2)		
C(2)–M(1)–C(5)	80.0(5)	81.6(3)	82.3(2)		
C(2)–M(1)–C(6)	88.7(5)	88.4(3)	89.9(2)		
C(5)–M(1)–C(6)	34.6(5)	34.9(3)	34.9(2)		
C1–2–M(1)–S(1) [b]	175.3	175.9	174.1		
C1–2–M(1)–P(2) [b]	94.5	94.7	94.8		
C5–6–M(1)–S(1) [c]	90.1	90.9	90.3		
C5–6–M(1)–P(2) [c]	174.3	175.1	173.7		
C1–2–M(1)–C5–6 [bc]	85.8	86.7	85.8		
M(1)–S(1)–P(1)	107.2(2)	105.2(1)	105.8(1)		
S(1)–P(1)–C(10)	110.5(4)	110.4(2)	110.8(2)	S(1)–P(1)–C(10)	115.9(1)
S(1)–P(1)–C(31)	107.0(4)	107.7(3)	107.4(2)	S(1)–P(1)–C(31)	112.3(1)
S(1)–P(1)–C(35)	110.1(6)	110.0(3)	108.6(2) [d]	S(1)–P(1)–C(41)	114.1(2)
C(10)–P(1)–C(31)	108.5(5)	107.8(3)	113.5(2)	C(10)–P(1)–C(31)	100.1(2)
C(10)–P(1)–C(35)	104.8(6)	105.8(3)	111.4(2) [e]	C(10)–P(1)–C(41)	107.8(2)
C(31)–P(1)–C(35)	115.9(7)	115.0(4)	104.7(2) [f]	C(31)–P(1)–C(41)	105.2(2)
M(1)–P(2)–C(10)	112.2(3)	111.7(2)	111.8(2)	Ru(1)–P(2)–C(10)	111.8(1)
M(1)–P(2)–C(11)	112.7(4)	111.4(2)	111.8(2)	Ru(1)–P(2)–C(11)	112.6(1)
M(1)–P(2)–C(21)	119.3(3)	120.7(2)	115.7(1)	Ru(1)–P(2)–C(21)	115.6(1)
C(10)–P(2)–C(11)	105.2(5)	104.3(3)	110.5(2)	C(10)–P(2)–C(11)	105.9(2)
C(10)–P(2)–C(21)	102.2(5)	102.2(3)	104.6(2)	C(10)–P(2)–C(21)	103.7(2)
C(11)–P(2)–C(21)	103.8(5)	105.0(3)	101.9(2)	C(11)–P(2)–C(21)	106.4(2)
P(1)–C(10)–P(2)	111.6(6)	110.9(3)	116.2(3)	P(1)–C(10)–P(2)	124.0(2)

[a] C1–6 represents the centre of the *p*-cymene ring. [b] C1–2 represents the centre of the C(1)–C(2) double bond. [c] C5–6 represents the centre of the C(5)–C(6) double bond. [d] S(1)–P(1)–C(41). [e] C(10)–P(1)–C(41). [f] C(31)–P(1)–C(41).

nation shifts of the anionic ligands are smaller, +51.8 (Rh) and +46.9 (Ir) ppm in [M(cod){$CH(PPh_2)$(P(S)Ph_2)-*P,S*}], and these trends hold for the other complexes in the study. The smaller values for iridium complexes are consistent with corresponding shifts in *cis* palladium (58–68 ppm) and platinum (42–50 ppm) complexes [9], and also with the normal trend of decreased shielding for ligands attached to heavier transition metals [36]. As is expected, the indirectly bound phosphorus of the P_B(S) group is less affected by coordination. Thus, the coordination shifts for P_B in [Rh(Lg){$CH_2(PPh_2)$(P(S)R_2)-*P,S*}]$^+$ cations range from 18 to 35 ppm, and it is interesting that in this case the values for corresponding iridium complexes are consistently somewhat larger, 22–40 ppm.

Changes in ^2J(P–P) on coordination of CH_2{PPh_2}{P(S)Ph_2} can arise from two causes: (i) coupling involving P^V atoms is generally smaller than similar couplings involving P^{III} [37,38]; and (ii) in complexes of the ligand, coupling through the P–C–P pathway may be enhanced or partially cancelled by contributions through the P–M–S–P pathway, depending on the relative signs of the two contributions [39]. In the present complexes, the couplings are sharply reduced by coordination but the actual magnitude of the reduction is very sensitive to the nature of the metal. Phosphorus–phosphorus coupling in the free ligand is 76 Hz, falling to 25 Hz in *cis*-[PtCl(PEt_3){CH_2(PPh_2)(P(S)Ph_2)-*P,S*}]$^+$. Values for [M(cod){$CH_2(PPh_2)$(P(S)Ph_2)-*P,S*}] are 51 (M = Rh) and 45 (M = Ir) Hz; and in the ruthenium complexes about 37 Hz in both [$RuCl_2$(benzene){$CH_2(PPh_2)$(P(S)Ph_2)-*P*}] and [RuCl(benzene){$CH_2(PPh_2)$(P(S)Ph_2)-*P,S*}]$^+$. If the value in the monodentate ruthenium complex indicates the reduction to be expected when P_A becomes formally 5-valent then the other changes must arise from contri-

butions through the metal pathway. The importance of the 'through metal' pathway is also demonstrated by the sensitivity of the P–P coupling to the other ligands on the metal. For example, the 25 Hz coupling in *cis*-$[PtCl(PEt_3)\{CH_2(PPh_2)(P(S)Ph_2)$-*P*,*S*$\}]^+$ with PEt_3 *trans* to S increases to 55 Hz in the *trans* isomer where Cl is *trans* to S [9]. Similar sensitivity is seen in Table 1 for the $[Rh(Lg)\{CH_2(PPh_2)(P(S)^tBu_2)$-*P*,*S*$\}]^+$ cations with P–P couplings ranging from 27 (Lg = $(CO)_2$) to 50 Hz (Lg = DPPM).

The other NMR change associated with the formation of the chelate complexes is a small deshielding, 2–4 ppm, of the central ligand carbon, C_A. Interestingly, in the monodentate ruthenium complex this carbon is actually shielded by about 12 ppm relative to the free ligand, but conversion to the *P*,*S*-coordinated derivative results in deshielding, showing that this effect is associated with formation of the chelate ring.

From the structural point of view, comparison of the monodentate ligand in **4** with the bidentate ligands in **1** and **2** shows that the ligand dimensions are essentially unchanged by formation of the chelate ring, except for a slight elongation (*ca.* 0.1 Å) of the P–S bond and some angle modifications required to actually form the ring.

Deprotonation of complexes $CH_2(PPh_2)(P(S)Ph_2)$ results in several changes in the NMR parameters:
(i) The central carbon is about 12 ppm more shielded;
(ii) the one-bond couplings from phosphorus to C_A are sharply increased;
(iii) the phosphorus–phosphorus coupling is sharply increased.

Structurally, these NMR changes are accompanied by shortening of the P–C bonds, by about 0.1 Å, and widening of the P–C_A–P angle, from 111 to 116°. We have previously discussed changes of this type caused by deprotonation of complexes of $CH_2\{P(S)Ph_2\}_2$ in terms of contributions from the possible resonance forms [33]. At first sight the major contributor to the actual structures of $[M(cod)\{CH(PR_2)(P(S)R_2)\}]^+$ cations might be assumed to be Structure **6a**.

However, there are several problems with this assumption. Although the comparison is not exact, the effect of a simple change of hybridization at the central carbon (**5a** → **6a**) may be evaluated by comparing $Ph_2P_ACH_2P_B(Se)Ph_2$ with $Ph_2P_AC(=CH_2)P_B(Se)Ph_2$ [38]. This change from sp^3 to sp^2 hybridization results in deshielding of C_A, from 34.6 to 142.6 ppm, increased coupling $J(P_A–C)$, −32 to −44 Hz, deshielding of P_A and P_B, −27.3 to −14.6 ppm and +30.9 to +39.2 ppm respectively, and relatively little change in $J(P_B–C)$ and J(P–P). These changes are not consistent with those seen in the present complexes. Moreover, alkene carbon resonances are normally deshielded and, for example, deprotonation of the central carbon of acetylacetone results in deshielding. By contrast, in simple phosphorus ylides [40], in $[CH\{P(S)Ph_2\}_2]^-$ complexes [33], and in the present $[CH(PPh_2)(P(S)Ph_2)]^-$ complexes, the carbons are more shielded than in corresponding saturated carbon compounds. Consequently in all of these phosphorus compounds it appears that the central carbon is relatively negatively charged, reflecting the importance of resonance forms **6b** and **6c** involving charge separation, rather than forms such as **6a** involving the development of a P=C double bond. Increased s-character at C_A, consistent with the wider P–C–P angle in the deprotonated complexes, accounts for the increased P–C coupling; and the shorter P–C bonds may be explained by enhanced ionic contributions to the bond strength.

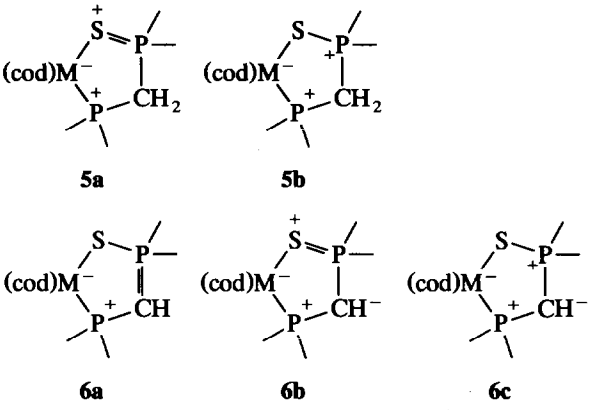

Scheme 3. Some possible resonance structures for $[M(cod)\{CH_2(PR_2)(P(S)R_2)$-*P*,*S*$\}]^+$ cations (**5**) and $[M(cod)\{CH(PR_2)(P(S)R_2)$-*P*,*S*$\}]$ complexes **6**

Acknowledgments

We thank the Natural Sciences and Engineering Research Council of Canada and the University of Victoria for research grants and Mrs C. Greenwood for recording NMR spectra.

References and notes

1 S. O. Grim and J. D. Mitchell, *Inorg. Chem., 16* (1977) 1762.
2 S. O. Grim and E. D. Walton, *Inorg. Chem., 19* (1980) 1982.
3 S. O. Grim, P. H. Smith, I. J. Colquhoun and W. McFarlane, *Inorg. Chem., 19* (1980) 3195.
4 I. J. Colquhoun, S. O. Grim, W. McFarlane, J. D. Mitchell and P. H. Smith, *Inorg. Chem., 20* (1981) 2516.
5 R. Colton and P. Panagiotidou, *Aust. J. Chem., 40* (1987) 13.
6 A. M. Bond, R. Colton and P. Panagiotidou, *Organometallics, 7* (1988) 1774.
7 M. Lusser and P. Peringer, *Inorg. Chim. Acta, 127* (1987) 151.
8 A. M. Bond, R. Colton and J. Ebner, *Inorg. Chem., 27* (1988) 1697.

9 D. E. Berry, J. Browning, K. R. Dixon and R. W. Hilts, *Can. J. Chem., 66* (1988) 1272.
10 C. A. Grygon, W. C. Fultz, A. L. Rheingold and J. L. Burmeister, *Inorg. Chim. Acta, 141* (1988) 205.
11 P. Peringer and J. Schwald, *J. Chem. Soc., Chem. Commun.*, (1986) 1625.
12 R. Colton, J. Ebner and B. F. Hoskins, *Inorg. Chem., 27* (1988) 1993.
13 R. Uson, A. Laguna, M. Laguna, M. N. Fraile, P. G. Jones and C. F. Erdbrugger, *J. Chem. Soc., Dalton Trans.*, (1989) 73.
14 R. W. Wegman, A. G. Abatjoglou and A. M. Harrison, *J. Chem. Soc., Chem. Commun.*, (1987) 1891.
15 R. S. Tanke and R. H. Crabtree, *J. Chem. Soc., Chem. Commun.*, (1990) 1056.
16 J. Browning, K. A. Beveridge, G. W. Bushnell and K. R. Dixon, *Inorg. Chem., 25* (1986) 1987.
17 J. Browning, K. R. Dixon, R. W. Hilts, N. J. Meanwell and F. Wang, *J. Organomet. Chem., 410* (1991) 289.
18 D. E. Berry, J. Browning, K. R. Dixon, R. W. Hilts and A. Pidcock, *Inorg. Chem., 31* (1992) 1479.
19 J. Browning, K. R. Dixon and R. W. Hilts, *Organometallics, 8* (1989) 552.
20 W. McFarlane and R. J. Wood, *J. Chem. Soc., Dalton Trans.*, (1972) 1397.
21 R. B. Johannsen, J. A. Ferreti and R. K. Harris, *J. Magn. Reson., 3* (1970) 84.
22 J. D. Swalen, in D. F. Detar, W. A. Benjamin (eds.), *Computer Programmes for Chemistry*. Vol. I, New York, 1968.
23 J. L. Herde, J. C. Lambert and C. V. Senoff, *Inorg. Synth., 15* (1974) 18.
24 G. Giordano and R. H. Crabtree, *Inorg. Synth., 19* (1979) 218.
25 R. A. Zelonka and M. C. Baird, *Can. J. Chem., 50* (1972) 3063.
26 M. A. Bennett and A. K. Smith, *J. Chem. Soc., Dalton Trans.*, (1974) 233.
27 Y. Le Page, E. J. Gabe and P. S. White, NRCCAD modification of the Enraf-Nonius program, Chemistry Division, National Research Council of Canada, Ottawa, Canada.
28 D. F. Grant and E. J. Gabe, *J. Appl. Cryst., 11* (1978) 114.
29 G. M. Sheldrick, SHELX-76, *A Computer Program for Crystal Structure Determination*, University of Cambridge, U.K., 1976.
30 L. J. Gabe, Y. Le Page, J. P. Charland, F. L. Lee and P. S. White, *J. Appl. Cryst., 22* (1989) 384.
31 C. K. Johnson, ORTEP *Report ORNL-3794*, Oak Ridge National Laboratory, Oak Ridge, TN, U.S.A., 1965.
32 D. T. Cromer and J. T. Waber, in J. A. Ibers and W. C. Hamilton (eds.), *International Tables for X-ray Crystallography*, Vol. IV., Kynoch Press, Birmingham, U.K. 1974.
33 J. Browning, G. W. Bushnell, K. R. Dixon and R. W. Hilts, *J. Organomet. Chem., 434* (1992) 241.
34 A. W. Coleman, H. Zhang, S. G. Bott, J. L. Atwood and P. H. Dixneuf, *J. Coord. Chem., 16* (1987) 9.
35 Supplementary material available from the authors: unit cell, data collection and refinement parameters for compounds **1–4** (Table S1, 2 pages); for **1**, anisotropic temperature factors for the heavy atoms (Table S2), interatomic distances (Table S3), bond angles (Table S4), selected intermolecular distances (Table S5) (4 pages), observed and calculated structure factor amplitudes (Table S6) (22 pages); corresponding tables for other crystals, **2** (Tables S7–S10, 17 pages), **3** (Tables S11–S18, 27 pages, including H atom parameters), **4** (Tables S19–S26, 32 pages, includes H-atom parameters).
36 K. R. Dixon, in J. Mason (ed.), *Multinuclear NMR*, Plenum Press, New York, 1987, p. 387.
37 Reference 36, pp. 388, 395.
38 I. J. Colquhoun and W. McFarlane, *J. Chem. Soc., Dalton Trans.*, (1982) 1915.
39 Reference 36, p. 396.
40 G. A. Gray, *J. Am. Chem. Soc., 95* (1973) 7736.